*Australian Meteorological and Oceanographic Journal 64* (2014) 147–158

# Seasonal climate summary southern hemisphere (spring 2013): Warmest Australian spring on record

**Tamika Tihema**
Queensland Regional Office, Bureau of Meteorolog , Australia

(Manuscript received June 2014)

Southern hemisphere circulation patterns and associated anomalies for the austral spring 2013 are reviewed, with emphasis given to the Pacific Basic climate indicators and Australian rainfall and temperature patterns. Pacific indicators were near neutral during spring. Sea surface temperatures were near average across much of the equatorial Pacific Ocean, however were warmer west of the Date Line and around Australia. The Indian Ocean Dipole returned to a neutral phase (though still displaying negative values) following large negative values during winter. The Southern Annular Mode continued in the negative phase it had entered in late winter, with large negative values observed in September, before weakening in November. Near-average spring rainfall was recorded for Australia nationally. A large area of the inland southeast was particularly dry; extending from west of the Great Dividing Range through southern Queensland, New South Wales, northern Victoria, South Australia and the southeast of the Northern Territory. In contrast much of northern Australia, Tasmania and the south of Western Australia received above average spring rainfall. It was the warmest spring on record for Australian in terms of both mean temperatures and maximum temperatures. Minimum temperatures were the fourth-warmest on record.

## Introduction

This summary reviews the southern hemisphere and equatorial climate patterns for spring 2013, with particular attention given to the Australasian and Pacific regions. The main sources of information for this report are analyses prepared by the Bureau of Meteorology's National Climate Centre and the Centre for Australian Weather and Climate Research (CAWCR).

## Pacific and Indian Basin climate indices

### Southern Oscillation Index

Troup Southern Oscillation Index[1] (SOI) for the period January 2009 to March 2014 is shown in Fig. 1, together with a five month weighted moving average. The SOI was weakly positive for September (+3.9), mildly negative for October (–1.9) and positive for November (+9.2), with spring remaining within the neutral range with an average value of +3.7. Spring 2012 had an average SOI of +3.0 (Reid et al., 2012) with the 2013 spring SOI slightly higher than the previous spring.

The spring mean sea level pressure (MSLP) values for Darwin were below average with 1010.0 hPa (average of 1010.5 hPa) and slightly above average for Tahiti with 1013.3 hPa (compared to the average of 1013.2 hPa). The monthly anomalies for Darwin in September, October and November were –0.4, 0.0 and –1.1 hPa respectively, and for Tahiti, +0.2, –0.3 and +0.3 hPa respectively.

### Composite monthly ENSO index (5VAR) // MEI

5VAR[2] is a composite monthly ENSO index, calculated as the standardised amplitude of the first principal component

[1] The Troup Southern Oscillation Index (Troup 1965) used in this article is ten times the standardised monthly anomaly of the difference in MSLP between Tahiti and Darwin. The calculation is based on a sixty-year climatology (1933–1992). The Darwin MSLP is provided by the Bureau of Meteorology, and the Tahiti MSLP is provided by Météo France inter-regional direction for French Polynesia.

[2] ENSO 5VAR was developed at the Bureau's National Climate Centre and is described in Kuleshov et al. 2009. The principal component analysis and standardisation of this ENSO index is performed over the period 1950–1999.

*Corresponding author address:* Tamika Tihema, Queensland Regional Office, Bureau of Meteorology, GPO Box 413, Brisbane Qld 4000, Australia.

Fig. 1. Southern Oscillation Index, from January 2009 to March 2014, together with a five-month binomially weighted moving average. Means and standard deviations used in the computation of the SOI are based on the period 1933–1992.

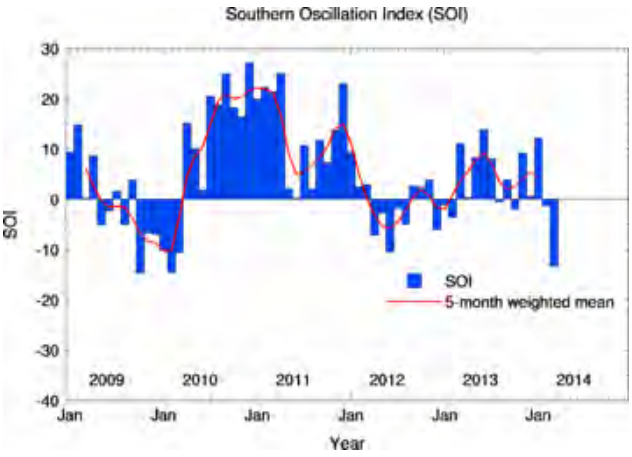


Fig. 2. 5VAR composite standardised monthly ENSO index from January 2007 to December 2013 together with a weighted three-month moving average. See text for details.

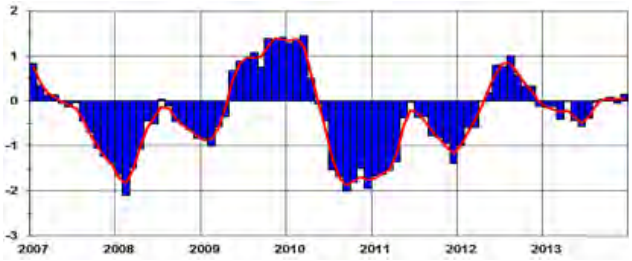


of monthly Darwin and Tahiti MSLP[3] and monthly NINO3, NINO3.4 and NINO4 sea-surface temperatures[4] (SSTs).

Monthly 5VAR values for the period January 2008 to December 2013, with a weighted three-month moving average, are shown in Fig. 2. For spring 2013, the 5VAR index was near neutral, with an average value of +0.02, and the values for September, October and November were +0.04, +0.08 and –0.05 respectively.

An increase in the 5VAR values indicates warming in the equatorial Pacific Ocean, while a decrease indicates cooling. Negative values in autumn and winter of 2013 were associated with a cooling of the equatorial Pacific since the latter part of 2012. The near-neutral values in spring 2013 indicate a return to neutral ocean temperatures.

The Multivariate ENSO Index[5] (MEI), produced by the US Climate Diagnostics Center, is derived from a number

[3] MSLP data obtained from www.bom.gov.au/climate/current/soihtm1.shtml. As previously mentioned, the Tahiti MSLP data are provided by Météo France inter-regional direction for French Polynesia.
[4] SST indices obtained from ftp://ftp.cpc.ncep.noaa.gov/wd52dg/data/indices/sstoi.indices.
[5] Multivariate ENSO Index obtained from www.esrl.noaa.gov/psd/people/klaus.wolter/MEI/table.html. The MEI is a standardised anomaly index described in Wolter and Timlin 1993, and 1998.

Fig. 3(a). OLR anomalies for spring 2013 (W m$^{-2}$). Base period is 1979–2000. The mapped region extends from 40°S to 40°N and from 70°E to 180°E.

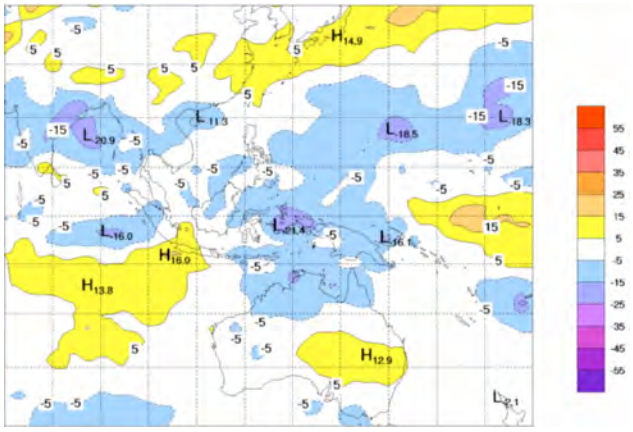

Fig. 3(b). OLR anomalies for spring 2013 (W m$^{-2}$). Base period 1979–2000. The mapped region extends over the southern hemisphere.

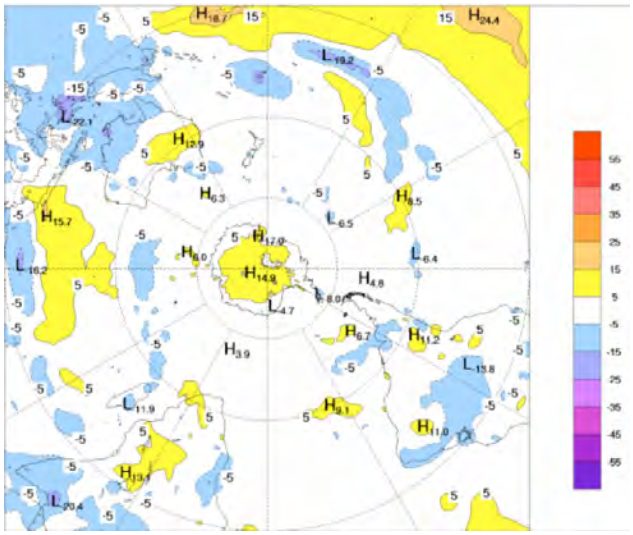

of atmospheric and oceanic parameters calculated as a two-month mean. As with 5VAR, significant negative anomalies in the MEI are usually associated with La Niña and, conversely, significant positive anomalies indicate El Niño. Monthly MEI values for spring 2013 were –0.19 (August–September), +0.094 (September–October) and –0.093 (October–November) with an average spring value of –0.063, representing neutral ENSO conditions.

### Outgoing long-wave radiation

Outgoing long-wave radiation (OLR) in the equatorial Pacific is a good indicator of changes in tropical convection patterns, with a general reduction in OLR (convection is enhanced) along the equator during an El Niño event, particularly near and east of the Date Line, whilst OLR is often increased (convection is supressed) along the equator during a La Niña, particularly near and west of the Date Line. Fig. 3(a) illustrates enhanced convection (negative OLR anomalies)

Fig. 4. Time-longitude section of daily-averaged OLR anomalies, averaged for 15°S to 15°N, for the period July 2013 to December 2013. Anomalies are with respect to a base period of 1979–2010.

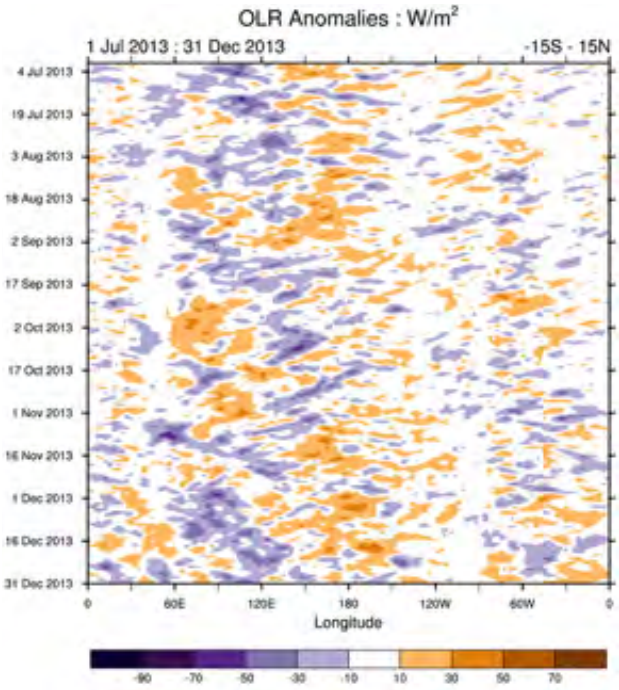


during spring 2013 over northern Australia along with areas in southern Australia. Supressed convection (positive OLR anomalies) was observed over central and east-central Australia, across the Indian Ocean and the equatorial Pacific Ocean. Anomalous positive values of the OLR were observed over the Antarctic region (Fig. 3(b)) for spring as well.

Standardised monthly anomalies[6] of OLR computed by the Climate Prediction Center, Washington, for an equatorial region ranging from 5°S to 5°N are calculated for September (+0.4), October (+0.2) and December (+0.8), with a spring average of +0.5.

The evolution of tropical convection anomalies along the equator with time is illustrated by the time-longitude section of daily-averaged OLR anomalies in Fig. 4.

## Madden-Julian Oscillation

The Madden-Julian Oscillation (MJO) is a tropical atmospheric anomaly which develops in the Indian Ocean and propagates eastwards into the Pacific Ocean (Donald et al. 2004). It takes approximately 30 to 60 days to reach the western Pacific, with a frequency of six to 12 events per year (Donald et al 2004). Tropical convective rainfall is associated with an active phase of the MJO. A description of the MJO index and the associated phases can be found in Wheeler and Hendon (2004).

The time-longitude section of daily-averaged OLR

[6] Obtained from www.cpc.ncep.noaa.gov/data/indices/olr.

Fig. 5. Phase-space representation of the MJO index for spring 2013. Daily values are shown with September in red, October in green and November in blue.

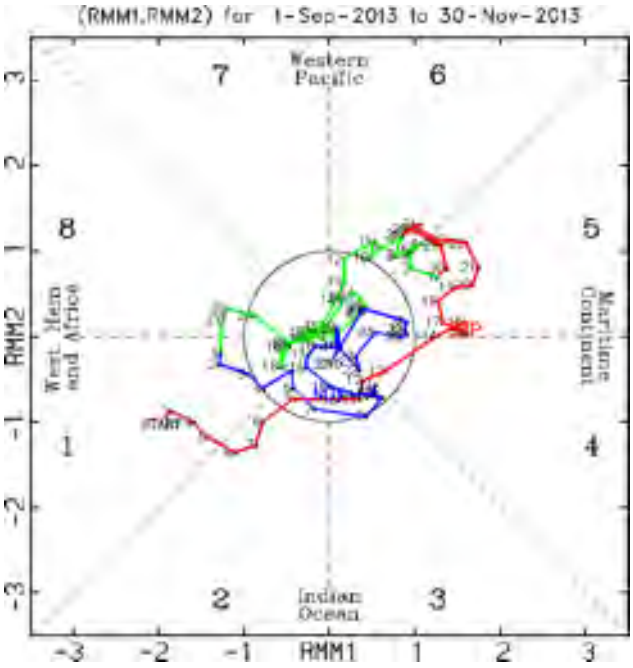


anomalies is shown in Fig. 4. The MJO was relatively inactive for around 40 days from July to mid-August. The MJO was active in phase one during late August before losing strength as it moved into phase two in early September. The MJO strengthened again from mid-September as it moved from the Maritime Continent into the Western Pacific (phases five and six). Activity from early October until the end of November generally fell within the circle defined as weak MJO activity, except for a short period of stronger activity in phases eight and one during the last days of October and first days of November. The phase-space representation of the MJO index for spring 2013 is shown in Fig. 5.

### Indian Ocean Dipole

The Indian Ocean Dipole (IOD) is the difference between the SSTs in the western (50°E to 70°W and 10°S to 10°N) and eastern (10°S to 0°N) equatorial Indian Ocean. The index is called the Dipole Mode Index (DMI), first described by Saji et al. (1999). A positive IOD is characterised by cooler-than-normal water in the tropical eastern Indian Ocean and warmer-than-normal water in the tropical western Indian Ocean. While a negative IOD is characterised by warmer-than-normal water in the tropical eastern Indian Ocean and warmer-than-normal water in the tropical western Indian Ocean. A positive IOD SST pattern has been shown to be associated with a decrease in rainfall over parts of central and southern Australia in austral winter and spring, whereas a negative IOD SST pattern is associated with higher rainfall.

Following a negative IOD event over the preceding winter, neutral values of the IOD prevailed during spring 2013. This followed the typical pattern in which an IOD event usually starts around May or June and peaks between

Fig. 6. Time series of the IOD for the period January 2010 to December 2013

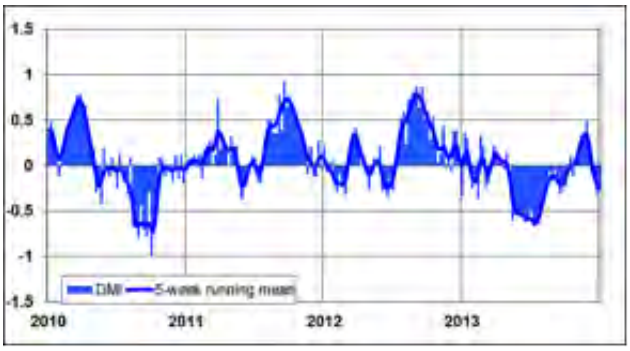


Fig. 7(a). Anomalies of global SST for spring 2013 (°C).

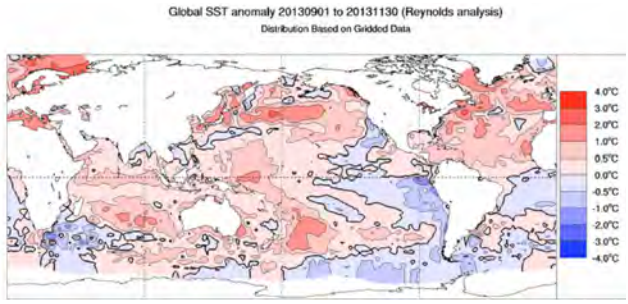


August and October, before rapidly decaying. The DMI values were mildly negative in September, near-neutral in October and mildly positive in November. Overall, spring had neutral values. The time series of the IOD for the period January 2010 to December 2013 is shown in Fig. 6.

## Oceanic patterns

### Sea surface temperatures

SST anomalies were obtained from the US National Oceanic and Atmospheric Administration (NOAA) Optimum Interpolation analyses (Reynolds et al. 2002). The base period is 1981–2010. Global SST anomalies for spring 2013 are shown in Fig. 7(a). Warm anomalies were present across the central southern Indian Ocean and along the equatorial region of the Indian Ocean. During spring, below-average SSTs were observed over the eastern half of the Pacific, although near-average SSTs were observed across most of the tropical Pacific during the middle of Octobe .

Spring SST deciles for the Australian region are shown in Fig. 7(b). Spring sea surface temperatures were above average around Australia, with those observed along the coast of the southern mainland the highest on record for spring. Large positive anomalies were also present on the east coast of Australia, and to a lesser extent along most of northern Australia.

Fig. 7(b). Deciles of SST for spring 2013 in the Australian region (°C).

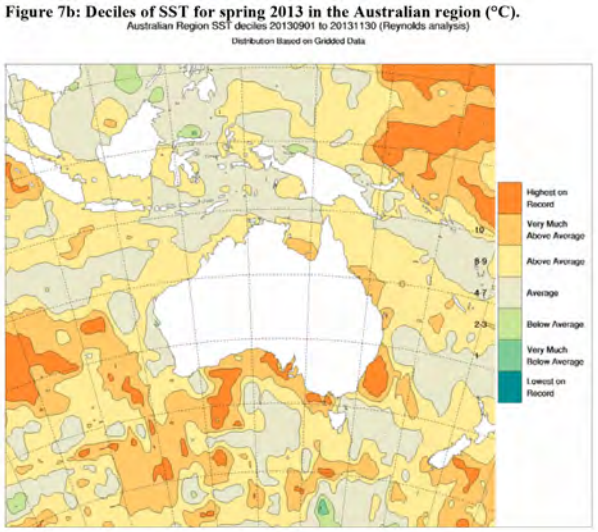


Fig. 8. Time-longitude section of the monthly anomalous depth of the 20 °C isotherm at the equator (2°S to 2°N) for January 2011 to December 2013. (Plot obtained from the TAO Project Office).

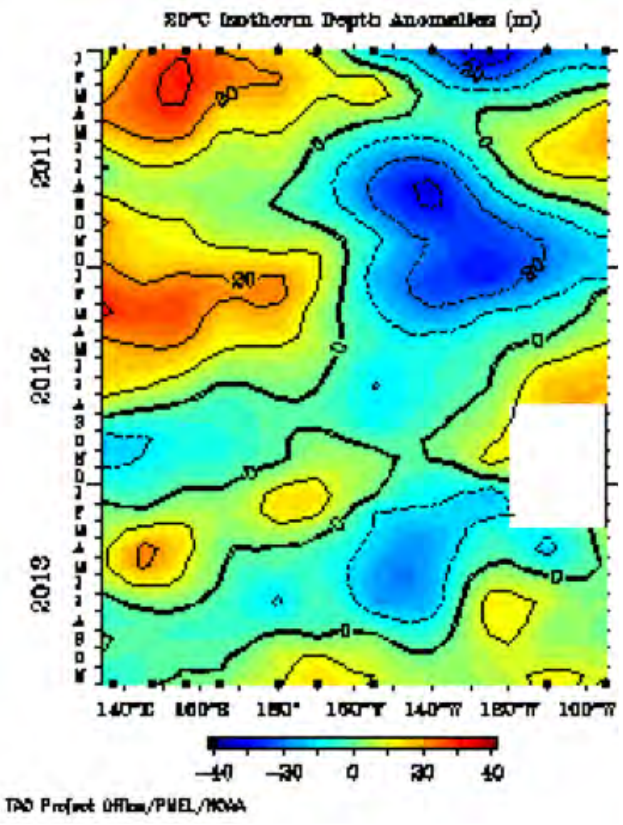

Fig. 9. Four-month August 2013 to November 2013 sequence of vertical sea subsurface temperature anomalies at the equator for the Pacific Ocean. The contour interval is 0.5 °C. (Plot obtained from CAWCR[8]).

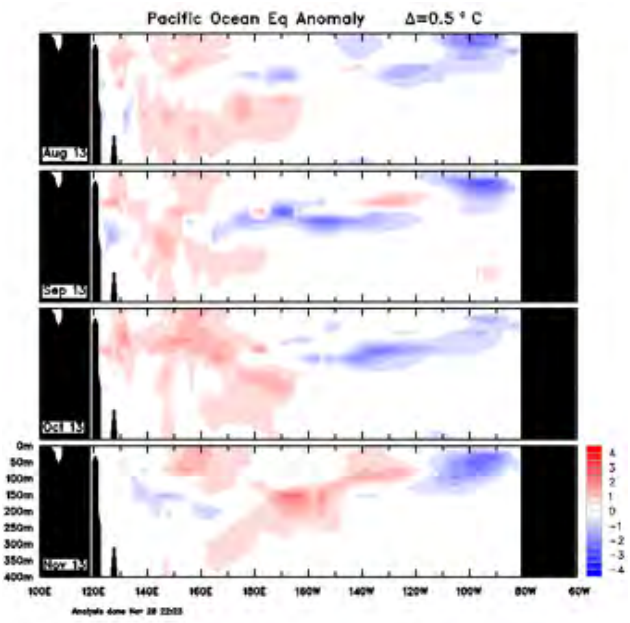


### Sub-surface patterns

The Hovmöller diagram for the 20 °C isotherm depth anomaly along the equator for January 2011 to November 2013 was obtained from the TAO Project Offic [7], and is shown in Fig. 8. The 20 °C isotherm depth is generally located close to the equatorial thermocline, which is the region of greatest temperature gradient with depth, and is the boundary between the warm near-surface and cold deep-ocean waters. The measurements of the 20 °C isotherm make a good proxy for the thermocline depth, with positive (negative) anomalies correspond to the 20 °C isotherm being deeper (shallower) than average. A shallow thermocline depth results in more cold water available for upwelling, and therefore a potential cooling of surface temperatures.

Figure 8 shows positive anomalies emerged east of the Date Line in mid-September, and continued to gradually warm into November. However, temperatures in sub-surface of the eastern Pacific remained close to neutral until warming somewhat in late spring.

Sub-surface temperature anomalies along the equator (in the area 2°S to 2°N) for January 2011 to November 2013 are shown in Fig. 9. Sub-surface temperatures in the western Pacific were generally warmer than average for the first two months of spring, and slightly warmer than those observed in the same area for spring 2012. Some eastward progression of warm sub-surface temperature anomalies can be seen across the three spring months, with temperatures near the Date Line warming slightly in October and further into the central Pacific in November. Anomalies in most of the central and eastern Pacific were negative in September, and sub-surface temperatures remained cooler than average in the far eastern equatorial Pacific sub-surface into November.

[7] Hovmöller plot obtained from www.pmel.noaa.gov/tao/jsdisplay

Fig. 10. Spring 2013 MSLP (hPa). The contour interval is 5 hPa.

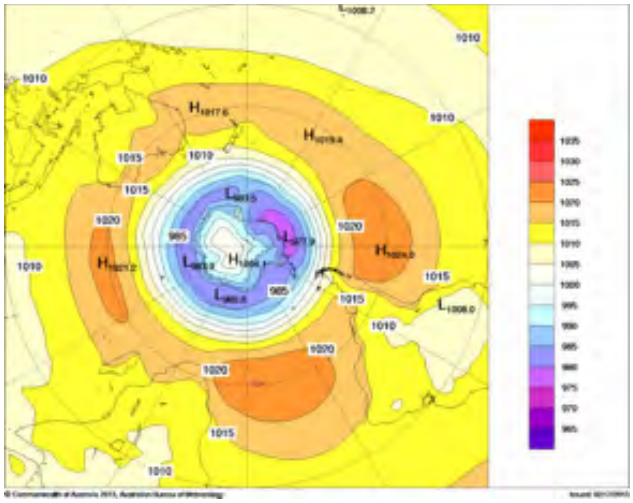

## Atmospheric patterns

### Surface analyses

The MSLP pattern for spring 2013 is shown in Fig. 10, computed using data from the 0000 UTC daily analyses of the Bureau of Meteorology's Australian Community Climate and Earth System Simulator (ACCESS) model[9]. The MSLP anomalies are shown in Fig. 11, relative to the 1979–2000 climatology obtained from the National Centers for Environmental Prediction (NCEP) II Reanalysis data (Kanamitsu et al. 2002). The MSLP anomaly field is not shown over areas of elevated topography (grey shading).

The spring 2013 pattern of MSLP was zonal at mid-to high-latitudes, with the strongest high pressure systems forming around 30°S. The strongest centres were located at 80°E over the central Indian Ocean with 1021.2 hPa and at 90°W with 1024 hPa. The lowest pressure measured 977.9 hPa over Antarctica between 150°W and 90°W.

Anomalously high pressure at mid-latitudes was evident between 130°W and 90°W. The highest anomaly in the southern hemisphere during spring 2013 fell within this band with 7.05 hPa above the long term average around 120°W and a broader region of anomalous high pressure 5.00 hPa above average stretching around West Antarctica. Most of Australia was under weak anomalously high pressure, with the highest anomaly of 2.36 hPa occurring over the Northern Territory, while much of the southern Indian Ocean between 110°E and 30°E and 30°S to 60°S recorded negative pressure anomalies, with the lowest 4.62 hPa below average.

[8] This and other analyses available from www.bom.gov.au/oceanography/oceantemp/pastanal.shtml

[9] For more information on the Bureau of Meteorology's ACCESS model, see www.bom.gov.au/nwp/doc/access/NWPData.shtml

Fig. 11. Spring 2013 MSLP anomalies (hPa), from a 1979–2000 climatology.

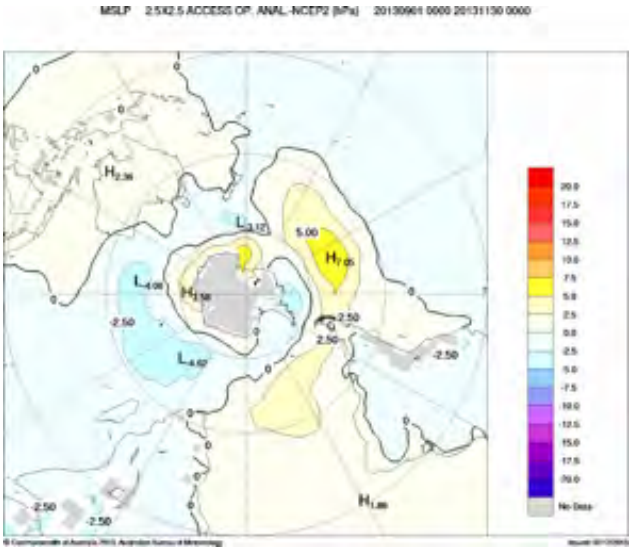

Fig. 12. Spring 2013 500 hPa mean geopotential height (gpm).

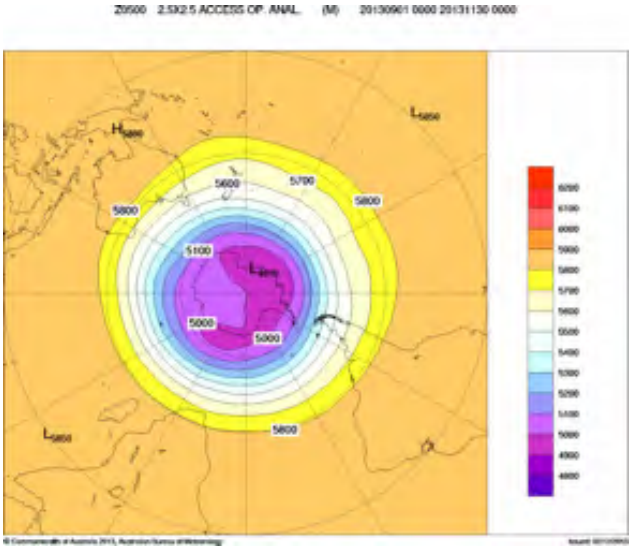

## Mid-tropospheric analyses

The 500 hPa geopotential height, which is a good indicator of the steering of surface synoptic systems across the southern hemisphere (measured in gpm), for spring 2013 is shown in Fig. 12. Figure 13 illustrates the associated anomalies. The spring 500 hPa geopotential height field in the southern hemisphere high-latitudes were characterised by zonal flo . The pattern of geopotential height anomalies are similar to the MSLP observations, however much larger positive anomalies were present at latitudes greater than 60°S at 500 hPa than at mean sea level, with a large positive anomaly of 154 gpm centred over Antarctica. Much of Australia (except Tasmania) was in an area of mildly positive high pressure, though mid-latitudes featured a large negative anomaly centred between 60°W and 30°W reaching more than +60 gpm.

Fig. 13. Spring 2013 500 hPa mean geopotential height anomalies (gpm), from a 1979–2000 climatology.

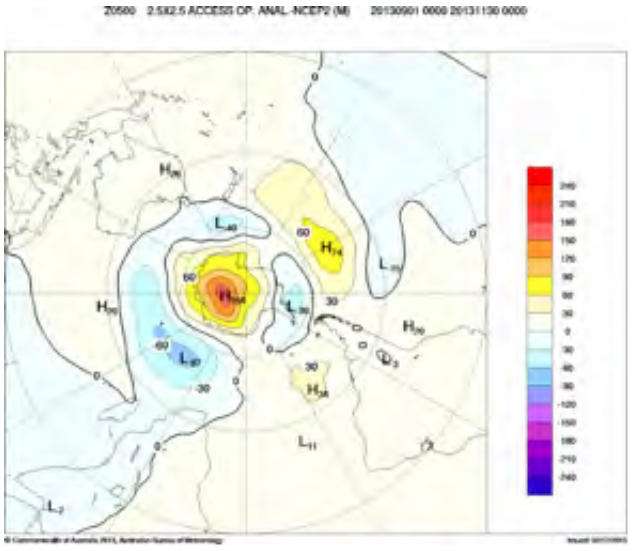

## Southern Annular Mode

The Southern Annular Mode (SAM), refers to the shift in the location of the belt of strong westerly winds in the mid-to-high latitudes of the southern hemisphere, with positive (negative) phases of SAM typically associated with negative (positive) anomalies in mid-latitudes. A poleward contraction (equatorward expansion) of the belt of westerly winds is a result of positive (negative) phases of SAM.

A strongly negative phase of SAM in late winter and spring (including the lowest August–October value of the SAM index since 1988), saw a shift in weather patterns as the subtropical ridge shifted further northwards, generating a westerly flow over southern Australia and enhancing rainfall in coastal areas exposed to the westerly winds. The negative phase of SAM continued to October, and returned to weak negative values by the end of spring. Further north, these westerlies produced hot and very dry conditions in New South Wales and Queensland.

The Climate Prediction Center produces a standardised monthly SAM index (Climate Prediction Center 2010)[10]; the September value was –1.66, October –0.46 and November +0.189. The September value was the lowest for any month during 2013.

## Winds

Low-level (850 hPa) wind anomalies are shown in Fig. 14 and upper-level (200 hPa) wind anomalies in Fig. 15 (derived from the 22-year NCEP II climatology). The lower-level wind anomalies indicate a mild westerly burst over the central Pacific in the mid-latitudes, while weak easterly wind bursts occurred over the central Indian Ocean. Upper-level northeasterly wind bursts were observed off the northeast

[10] For more information on the SAM index from the Climate Prediction Center (NOAA), see www.cpc.ncep.noaa.gov/products/precip/CWlink/daily_ao_index/aao/aao.shtml

Fig. 14. Spring 2013 850 hPa vector wind anomalies (m $s^{-1}$). The anomaly field is not shown over areas of elevated topography.

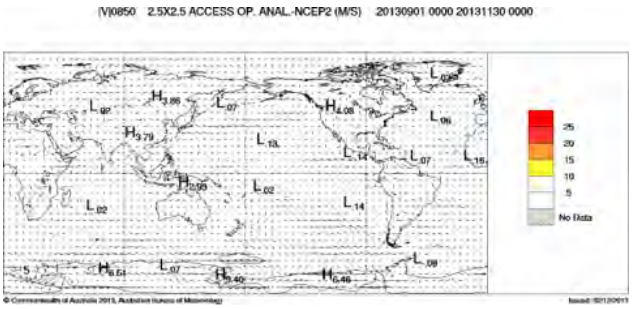


coast of Australia and stronger westerlies across most of the Southern Ocean, particularly near the Australian coast. Anti-cyclonic wind bursts were observed over mainland Australia and strong westerlies in the mid-latitude eastern Pacific reaching northern Chile

## Australian region

### Rainfall

Australian spring rainfall totals for 2013 are shown in Fig. 16 and spring 2013 deciles are shown in Fig. 17. The deciles are calculated with respect to gridded rainfall data for all spring periods between 1900 and 2013.

Averaged across Australia, spring rainfall was five per cent below the 1961–1990 average of 72 mm (see Table 1). Spring was particularly dry across the interior and inland of the eastern States, including New South Wales west of the Great Dividing Range, western and southern Queensland, and the southern half of the Northern Territory and most of South Australia, with these areas recording below-average rainfall. State-wide, rainfall for South Australia was 13 mm (55 per cent) below average and 31 mm (31 per cent) below average in New South Wales. More than half of South Australia recorded rainfall in the lowest ten per cent of records and for the State as a whole, spring rainfall was the thirteenth-lowest on record. Just under one per cent (0.78 per cent) of Australia recorded its lowest rainfall on record, 6.8 per cent was in severe deficiency (lowest five per cent of spring records) and 19.3 per cent of the country was in the lowest decile (driest ten per cent of spring records).

In contrast, Tasmania and the tropical north, southwest Western Australia along with eastern Western Australia, the southeast mainland received above-average rainfall in spring. The area-averaged totals for Tasmania, Western Australia and the Northern Territory were 33 per cent, 27 per cent and nine per cent above the 1961–1990 mean respectively. An area totalling 0.15 per cent of Australia had its highest spring rainfall on record. Regionally, 0.23 per cent of the Northern Territory, 0.43 per cent of Queensland and 1.81 per cent of Tasmania received record-high spring rainfall.

Negative SAM values in September and October saw

Fig. 15. Spring 2013 200 hPa vector wind anomalies (m $s^{-1}$).

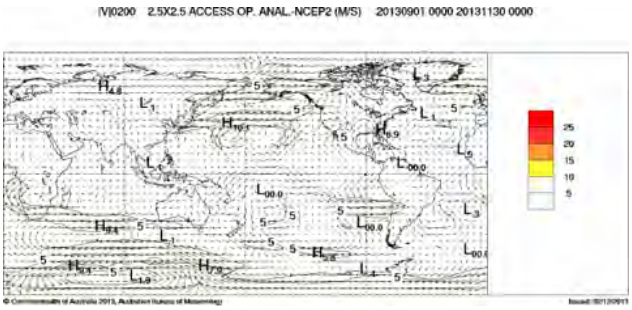


Fig. 16. Spring 2013 rainfall totals (mm) for Australia.

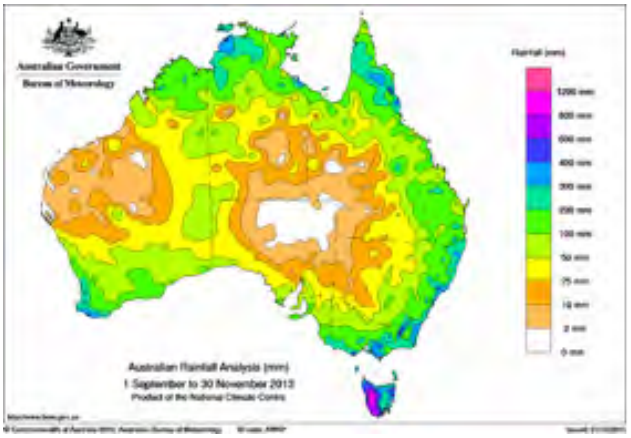


Fig. 17. Spring 2013 rainfall deciles for Australia: decile ranges based on grid-point values over the spring 1900–2013.

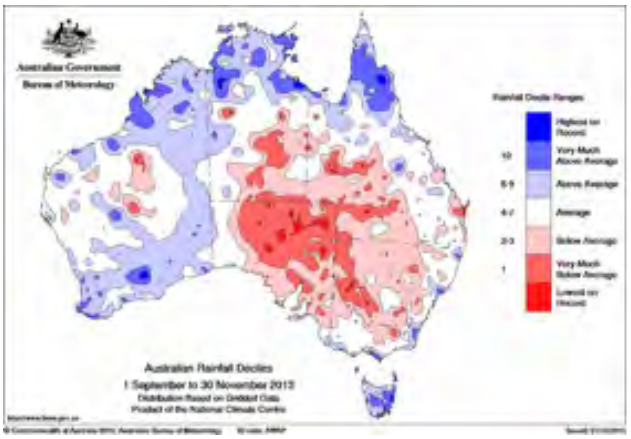


a northward shift in the sub-tropical ridge, resulting in enhanced rainfall in the southern part of Western Australia, the exposed coastal strip along the coast of Victoria and parts of Tasmania. Southern Western Australia recorded above-average rainfall with the majority of the region's rain falling in September, while numerous thunderstorms throughout October brought above-average rainfall across the northwest.

Tropical cyclone *Alessia* was the first cyclone of the Australian region for the 2013–14 tropical cyclone season. The system tracked just north of the Kimberley coast and made landfall near Daly River Mouth in the Northern

Table 1. Summary of the seasonal rainfall ranks and extremes on a national and State basis for spring 2013. The ranking in the last column goes from 1 (lowest) to 114 (highest) and is calculated over the years 1900–2013.

| *Region* | *Highest seasonal total (mm)* | *Lowest seasonal total (mm)* | *Highest daily total (mm)* | *Area-averaged rainfall (mm)* | *Rank of area-averaged rainfall* | *% difference from mean* |
|---|---|---|---|---|---|---|
| Australia | 963.7 mm at Strathgordon Village (Tas) | 0.0 mm at several locations | 267.4 mm at Bowen Airport, 23 Nov (Qld) | 69 | 62 | –5 |
| Queensland | 630.2 mm at Whyanbeel Valley | 0.0 mm at several locations | 267.4 mm at Bowen Airport, 23 Nov | 81 | 61 | –5 |
| New South Wales | 625.8 mm at Perisher Valley | | 220.4 mm at Robertson (The Pie Shop), 17 Sep | 86 | 31 | –31 |
| Victoria | 684.4 mm at Wyelangta | 34.2 mm at Mildura Airport | 76.2 mm at Reeves Knob, 12 Nov | 156 | 40 | –14 |
| Tasmania | 963.7 mm at Strathgordon Village | 178.4 mm at Mount Morriston (Macquarie River) | 258.0 mm at Gray (Haven of Hope), 13 Nov | 485 | 105 | +33 |
| South Australia | 238.4 mm at Mount Schank (Jethia) | 0.0 mm at Moomba Airport | 51.2 mm at Penola Post Office, 17 Se | 23 | 13 | –55 |
| Western Australia | 438.7 mm at Northcliffe | 0.0 at Wallanreenya | 120.0 mm at Emma Gorge, 22 Nov | 52 | 89 | +27 |
| Northern Territory | 715.2 mm at Stokes Hill | 0.0 at several locations | 200.4 mm at McArthur River Mine Airport, 28 Nov | 73 | 78 | +9 |

Table 2. Percentage areas in different categories for spring 2013 rainfall. 'Severe deficiency' denotes rainfall at or below the 5th percentile. Areas in 'decile 1' include those in 'severe deficiency', which in turn include those which are 'lowest on record'. Areas in 'decile 10' include those which are 'highest on record'. Percentage areas of highest and lowest on record are given to two decimal places because of the small quantities involved; other percentage areas to one decimal place.

| *Region* | *Lowest on record* | *Severe deficiency* | *Decile 1* | *Decile 10* | *Highest on record* |
|---|---|---|---|---|---|
| Australia | 0.78 | 6.8 | 13.4 | 7.0 | 0.15 |
| Queensland | 0.16 | 1.7 | 9.0 | 9.5 | 0.43 |
| New South Wales | 0.79 | 7.1 | 17.5 | 0.7 | 0.00 |
| Victoria | 0.00 | 0.0 | 2.2 | 1.6 | 0.00 |
| Tasmania | 0.00 | 0.0 | 0.0 | 41.4 | 1.81 |
| South Australia | 2.63 | 34.3 | 53.0 | 0.0 | 0.00 |
| Western Australia | 0.00 | 0.1 | 0.5 | 7.4 | 0.00 |
| Northern Territory | 1.87 | 6.9 | 13.9 | 11.3 | 0.23 |

Territory. This saw an early start to the northern wet season at the end of November, and contributed to the above-average spring rainfall across the Kimberley region, through the Top End and Cape York Peninsula.

### Drought

The rainfall deficiencies for the 14-month and 20-month period ending in November 2013 are shown in Fig. 18 and 19 respectively.

Rainfall deficits for the 14-month (October 2012 to November 2013 showed serious to severe deficiencies (lowest ten per cent and five per cent of records) were in place for much of central and western Queensland and the adjacent New South Wales border region.

The longer-term deficiencies for the 20-month (April 2012 to November 2013) period showed serious to severe deficiencies between Geraldton and Shark Bay on the west coast of Western Australia, across parts of the Nullabor

Fig. 18. Rainfall Deficiencies for the 14-month period (1 Oct 2012 to 30 November 2013).

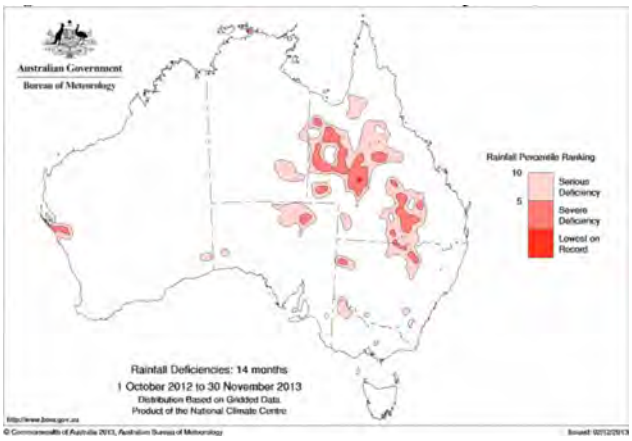


Fig. 19. Rainfall Deficiencies for the 20-month period (1 Apr 2012 to 30 November 2013).

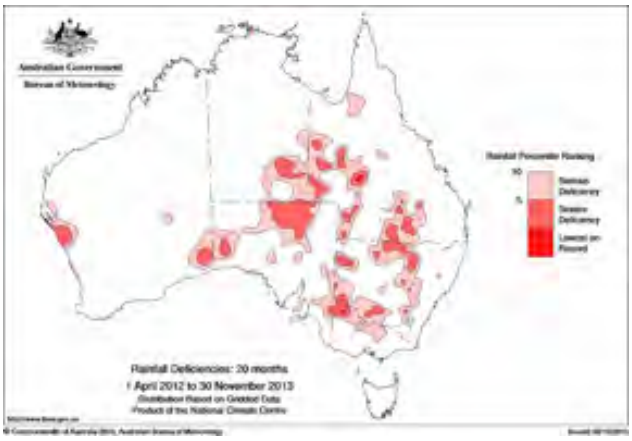


Fig. 20. Spring 2013 maximum temperature anomalies (°C).

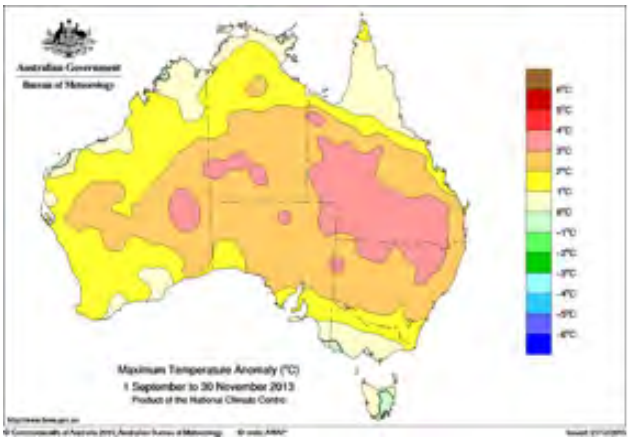


Fig. 21. Spring 2013 maximum temperature deciles: decile ranges based on grid-point values over the springs 1911–2013.

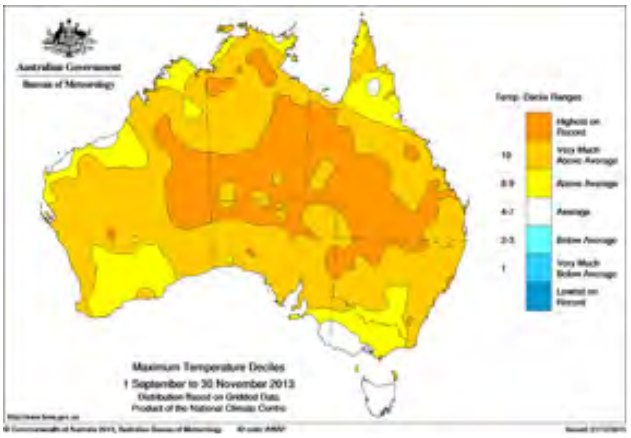


Fig. 22. Spring 2013 minimum temperature anomalies (°C).

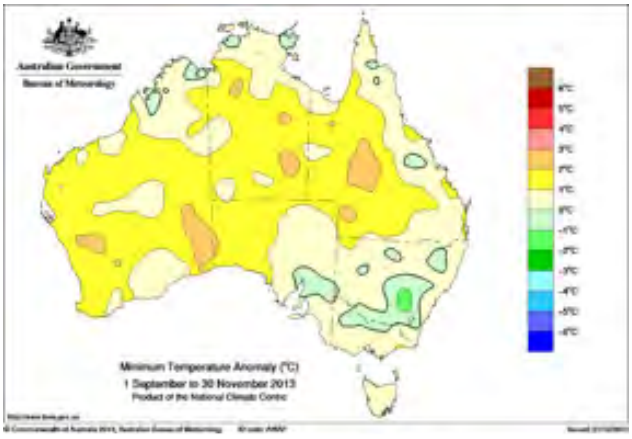


Fig. 23. Spring 2013 minimum temperature deciles: decile ranges based on grid-point values over the springs 1911–2013.

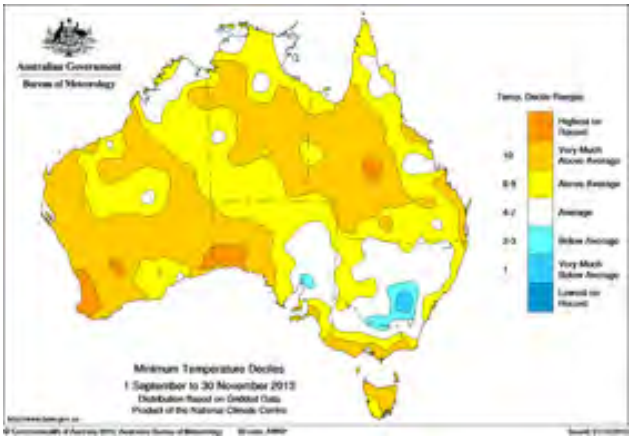

Table 3. Percentage areas in different categories for spring 2013. Areas in 'decile 1' include those which are 'lowest on record'. Areas in 'decile 10' include those which are 'highest on record'. Percentage areas of highest and lowest on record are given to two decimal places because of the small quantities involved; other percentage areas to one decimal place. Grid-point deciles calculated with respect to 1911–2013.

| *Region* | *Maximum temperature* | | | | *Minimum temperature* | | | |
|---|---|---|---|---|---|---|---|---|
| *Region* | *Lowest on record* | *Decile 1* | *Decile 10* | *Highest on record* | *Lowest on record* | *Decile 1* | *Decile 10* | *Highest on record* |
| Australia | 0.00 | 0.0 | 82.3 | 28.46 | 0.00 | 0.3 | 46.0 | 2.51 |
| Queensland | 0.00 | 0.0 | 87.5 | 47.02 | 0.00 | 0.0 | 53.8 | 2.06 |
| New South Wales | 0.00 | 0.0 | 87.9 | 18.58 | 0.00 | 3.1 | 0.7 | 0.00 |
| Victoria | 0.00 | 0.0 | 10.2 | 0.00 | 0.00 | 0.0 | 29.7 | 0.00 |
| Tasmania | 0.00 | 0.0 | 0.0 | 0.00 | 0.00 | 0.0 | 75.9 | 0.00 |
| South Australia | 0.00 | 0.0 | 95.8 | 24.78 | 0.00 | 0.0 | 32.1 | 6.32 |
| Western Australia | 0.00 | 0.0 | 73.2 | 13.56 | 0.00 | 0.0 | 61.8 | 3.74 |
| Northern Territory | 0.00 | 0.0 | 95.9 | 47.65 | 0.00 | 0.0 | 45.8 | 0.00 |

Table 4. Summary of the seasonal maximum temperature ranks and extremes on a national and State basis for spring 2013. The ranking in the last column goes from 1 (lowest) to 104 (highest) and is calculated over the years 1950–2013[11].

| *Region* | *Highest seasonal mean maximum (°C)* | *Lowest seasonal mean maximum (°C)* | *Highest daily temperature (°C)* | *Lowest daily maximum temperature (°C)* | *Area-averaged temperature anomaly (°C)* | *Rank of area-averaged temperature anomaly* |
|---|---|---|---|---|---|---|
| Australia | 40.5 at Fitzroy Crossing (WA) | 7.2 at Mount Wellington (Tas) | 46.4 at Roebourne, 5 Nov (WA) | –3.1 at Mount Wellington, 11 Sep (Tas) | 2.06 | 104 |
| Queensland | 38.9 at Century Mine | 24.5 at Applethorpe | 45.2 at Birdsville, 28 Nov | 14.5 at Stanthorpe, 16 Sep | 2.41 | 104 |
| New South Wales | 32.6 at Mungindi | 8.2 at Thredbo | 42.5 at Wilcannia, 21 Oct | –1.0 at Thredbo on 11 Sep and 24 Oct | 2.75 | 102 |
| Victoria | 26.2 at Mildura | 7.6 at Mount Hotham | 38.0 at Charlton, 27 Nov | –1.9 at Mount Baw Baw, 27 Oct | 1.09 | 87 |
| Tasmania | 18.2 at Friendly Beaches | 7.2 at Mount Wellington | 30.7 at Friendly Beaches 20 Oct | –3.1 at Mount Wellington, 11 Sep | 0.04 | =57.5 |
| South Australia | 33.0 at Oodnadatta | 17.1 at Mount Lofty | 43.9 at Moomba Airport, 28 Nov | 9.2 at Mount Lofty, 10 Sep | 2.56 | 102 |
| Western Australia | 40.5 at Fitzroy Crossing | 19.3 at Cape Leeuwin | 46.4 at Roebourne, 5 Nov | 11.2 at Rocky Gully, 19 Oct | 1.58 | 102 |
| Northern Territory | 38.9 at Bradshaw | 30.6 at McCluer Island | 43.3 at Douglas River on 16 Oct, and Rabbit Flat on 10 Oct | 23.3 at Kulgera on 14 Oct | 2.01 | 104 |

Plain, a large area encompassing most of far northern South Australia, the southeastern Northern Territory and southwestern Queensland, and across eastern Australia west of the Great Dividing Range from northwestern Victoria well into southern Queensland.

### Temperature

Fig. 20 and 22 show maximum and minimum temperature anomalies for spring 2013. Seasonal anomalies are calculated with respect to the 1961–1990 period, and use all stations for which an elevation is available. Station normals have been estimated using gridded climatologies for those stations with insufficient data within the 1961–1990 period to calculate a station normal directly. Figures 21 and 23 show maximum

Table 4. Summary of the seasonal maximum temperature ranks and extremes on a national and State basis for spring 2013. The ranking in the last column goes from 1 (lowest) to 104 (highest) and is calculated over the years 1950–2013[11].

| *Region* | *Highest seasonal mean minimum (°C)* | *Lowest seasonal mean minimum (°C)* | *Highest daily minimum temperature (°C)* | *Lowest daily temperature (°C)* | *Area-averaged temperature anomaly (°C)* | *Rank of area-averaged temperature anomaly* |
|---|---|---|---|---|---|---|
| Australia | 28.0 at Tibooburra (NSW) | 0.3 at Thredbo (NSW) and Mount Wellington (Tas) | 31.8 at Argyle, 17 Nov (WA) | –11.6 at Perisher Valley, 13 Sep (NSW) | 1.07 | 101 |
| Queensland | 25.0 at Sweers Island | 9.2 at Applethorpe | 29.5 at Croydon, 19 Oct and Windorah on 28 Nov | 0.0 at Stanthorpe on 4 Oct and Quilpie on 18 Oct | 1.22 | 100 |
| New South Wales | 28.0 at Tibooburra | 0.3 at Thredbo | 28.0 at Tibooburra on 22 Oct and Fowlers Gap on 28 Nov | –11.6 at Perisher Valley, 13 Sep | 0.48 | 76 |
| Victoria | 23.6 at Echuca on | 0.8 at Mount Hotham | 23.6 at Echuca, 28 Nov | –8.1 at Mount Hotham, 13 Sep | 0.52 | 90 |
| Tasmania | 10.5 at Swan Island | 0.3 at Mount Wellington | 16.6 at Friendly Beaches, 20 Oct | –8.8 at Liawenee, 13 Sep | 0.65 | 97 |
| South Australia | 16.1 at Oodnadatta | 5.9 at Yongala | 26.5 at Marla Police Station, 26 Nov | –2.4 at Keith (Munkora), 10 Nov | 0.97 | =94.5 |
| Western Australia | 26.8 at Troughton Island | 7.8 at Newdegate | 31.8 at Argyle, 17 Nov | –5.0 at Eyre on 14 Oct | 1.12 | 102 |
| Northern Territory | 26.2 at McCluer Island | 26.2 at McCluer Island | 30.2 at Wave Hill, 10 Oct | 3.7 at Yulara Airport, 20 Sep | 1.35 | 99 |

and minimum temperature deciles calculated using monthly temperature analyses from 1911 to 2013.

Spring 2013 was the warmest on record for maximum temperatures for Australia as a whole. Both Queensland and the Northern Territory also had record high maxima. New South Wales, South Australia and Western Australia had their third warmest maximum temperatures on record. Table 4 shows the summary of the seasonal maximum temperature, ranks and extremes on a national and State basis for spring 2013. The ranking in the last column goes from 1 (lowest) to 104 (highest).

The maximum temperature anomaly for Australia was +2.06 °C, surpassing the previous 2006 record by 0.23 °C. Queensland had an anomaly of +2.04 °C, and the Northern Territory had an anomaly of +2.01 °C, both record-warmest spring maxima. New South Wales, South Australia and Western Australia were all third-warmest on record, with anomalies of +2.75 °C, +2.56 °C and +1.58 °C respectively.

September was exceptionally warm, with both area-averaged maximum and minimum temperatures ranking as the highest on record. September had unusually hot days, with the area-average monthly maximum temperatures 3.41 °C above average Australia-wide, and monthly minimum temperatures 2.09 °C above average. The record September temperatures follow Australia's second-warmest winter on record for maximum temperatures (see Special Climate Statement 46).

Table 3 shows the percentage areas of maximum temperatures in different categories for spring 2013, including lowest and highest on record. Twenty-eight per cent of Australia had record-high maximum temperatures in spring. Around 47 per cent of Queensland was the highest on record, with a similar area in the Northern Territory also having record-high spring maxima. Nearly 82 per cent of Australia had very-much-above-average maximum temperatures in spring.

Maximum temperatures were highest on record for a broad area extending from the central west of Western Australia through the central interior and into western and southern inland Queensland and northern border areas of New South Wales, and a small area of the east coast north of Newcastle. They were near-average through Tasmania, southwestern Victoria and southeastern South Australia, and above to highest on record over the rest of Australia. Figure 21 shows spring 2013 minimum temperature deciles,

[11] A high-quality subset of the temperature network is used to calculate the spatial averages and rankings shown in Table 4 (maximum temperature) and Table 5 (minimum temperature). These averages are available from 1950 to the present. As the anomaly averages in the tables are only retained to two decimal places, tied rankings are possible.

including areas of above (and below) to very much above (and below) average, highest and lowest on record.

Minimum temperatures were above average for Australia as a whole, and the fourth-highest on record with an anomaly of +1.07 °C. Western Australia had its third-warmest spring minima on record (1.12 °C above average), Queensland had its fifth-warmest (1.22 °C above average) and the Northern Territory with its sixth-warmest and an anomaly of +1.35 °C. Table 5 shows the summary of the seasonal minimum temperature, ranks and extremes on a national and State basis for spring 2013. The ranking in the last column goes from one (lowest) to 104 (highest).

Table 3 shows the percentage areas of minimum temperatures in different categories, including lowest and highest on record for spring 2013. Area-averaged, around 2.5 per cent of Australia had record-warm spring minima. Over six per cent of South Australia, three per cent of Western Australia and two per cent of Queensland also had record-high minimum temperatures.

Minimum temperatures were above to very much above average across the Northern Territory, most of Western Australia and Queensland, western and southeastern South Australia, southern Victoria, parts of far western and coastal New South Wales and Tasmania. Northern Victoria, the remainder of New South Wales and eastern South Australia recorded near-average minima. Below-average minima were recorded in a large area covering the South West Slopes district in New South Wales and a small area in near Port Augusta in South Australia. Figure 23 illustrates the spatial distribution of spring 2013 minimum temperature deciles, including areas of average to very much above average, and highest on record.

## References


Donald, A., Meinke, H., Power, P., Wheeler, M., and Ribbe, J. 2004. Forecasting the Madden-Julian Oscillation and the application for risk management. In: 4th International Crop Science Congress, 26 September – 01 October 2004, Brisbane, Australia

Kanamitsu, M., Ebisuzaki, W., Woollen, J., Yang, S.-K, Hnilo, J.J., Fiorino, M. and Potter, G.L. 2002. NCEP-DOE AMIP-II Reanalysis (R-2). *Bull. Amer. Meteor. Soc., 83,* 1631–43.

Kuleshov, Y. Qi, L., Fawcett, R., Jones, D. 2009. 'Improving preparedness to natural hazards: Tropical cyclone prediction for the Southern Hemisphere,' in: Gan, J. (Ed.), Advances in Geosciences, *Vol. 12 Ocean Science,* World Scientific Publishing, Singapore, 127–43

Reid, P.A., Tully, M.B., Klekociuk, A.R., Krummel, P.B. and Rhodes, S.K. 2013. Seasonal climate summary southern hemisphere (spring 2013): warmer and drier across much of Australia, along with a new southern hemisphere sea ice extent record. *Aust. Met. Oceanogr. J., 63,* 472–42

Reynolds, R.W., Rayner, N.A., Smith, T.M., Stokes, D.C. and Wang, W. 2002. An improved in situ and satellite SST analysis for climate. *J. Clim., 15,* 1609–25.

Saji, N.H., Goswami, B.N., Vinayachandran, P.N. and Yamagata, T. 1999. A dipole mode in the tropical Indian Ocean. *Nature, 401,* 360–3.

Troup, A.J. 1965. The Southern Oscillation. *Q. J. R. Meteorol. Soc., 91,* 490–506.

Wheeler, M.C., and Hendon H.H. 2004. An All-Season Real-Time Multivariate MJO Index: Development of an Index for Monitoring and Prediction. *Mon.Weather Rev., 132,* 1917–32.

Wolter, K. and Timlin, M.S. 1993. Monitoring ENSO in COADS with a seasonally adjusted principal component index. Proc. Of the 17th Climate Diagnostics Workshop, Norman, OK, NOAA/NMC/CAC, NSSL, Oklahoma Clim. Survey, CIMMS and the School of Meteorology, Univ. of Oklahoma, 52–7.

Wolter, K. and Timlin, M.S. 1998. Measuring the strength of ENSO – how does 1997/98 rank?, *Weather, 53,* 315–24.